Monthly Notices of the ROYAL ASTRONOMICAL SOCIETY

MNRAS **484,** 5785–5790 (2019)
Advance Access publication 2019 February 11

doi:10.1093/mnras/stz395

Detection of a quasi-periodic oscillation in γ-ray light curve of the high-redshift blazar B2 1520+31

Alok C. Gupta,[1★] Ashutosh Tripathi,[2★] Paul J. Wiita,[3★] Pankaj Kushwaha,[4] Zhongli Zhang[5] and Cosimo Bambi[2,6]

[1]*Aryabhatta Research Institute of Observational Sciences (ARIES), Manora Peak, Nainital 263 001, India*
[2]*Center for Field Theory and Particle Physics and Department of Physics, Fudan University, 220 Handan Road, Shanghai 200433, China*
[3]*Department of Physics, The College of New Jersey, PO Box 7718, Ewing, NJ 08628-0718, USA*
[4]*Department of Astronomy (IAG-USP), University of Sao Paulo, Sao Paulo 05508-090, Brazil*
[5]*Shanghai Astronomical Observatory, Chinese Academy of Sciences, 80 Nandan Road, Shanghai 200030, China*
[6]*Theoretical Astrophysics, Eberhard-Karls-Universität Tübingen, D-72076 Tübingen, Germany*

Accepted 2019 February 4. Received 2019 January 19; in original form 2018 October 22

ABSTRACT

We detected a possible quasi-periodic oscillation (QPO) of ∼71 d in the 0.1–300 GeV γ-ray *Fermi*-Large Area Telescope light curve of the high-redshift flat spectrum radio quasar B2 1520+31. We identify and confirm that quasi-period by Lomb–Scargle periodogram and weighted wavelet Z-transform analyses. Using this QPO period, and assuming it originates from accretion disc fluctuations at the innermost stable circular orbit, we estimate the central supermassive black hole mass to range between $\sim 5.4 \times 10^9$ M$_\odot$ for a non-rotating black hole and $\sim 3.4 \times 10^{10}$ M$_\odot$ for a maximally rotating black hole. We briefly discuss other possible radio-loud active galactic nuclei emission models capable of producing a γ-ray QPO of such a period in a blazar.

Key words: radiation mechanisms: non-thermal – galaxies: jets – quasars: general – quasars: individual: B2 1520+31 – gamma-rays: galaxies.

1 INTRODUCTION

Active galactic nuclei (AGNs) powered by accreting black holes (BHs) with masses of 10^6–10^{10} M$_\odot$ have several similarities to scaled-up galactic X-ray emitting BH binaries. In both BH and neutron star binaries in our and nearby galaxies, the presence of quasi-periodic oscillations (QPOs) in the time series data, or light curves, is fairly common (e.g. Remillard & McClintock 2006). But it is quite rare to detect QPOs in the time series data of AGN.

Blazars are a subclass of radio-loud AGN with their relativistic jets aligned along the observer's line of sight. They have been empirically classified further into BL Lac objects (BLLs) and flat spectrum radio quasars (FSRQs) based on the strength of optical emission lines, where the former show no or very weak ones while the latter have prominent broad lines. All blazars exhibit highly variable fluxes across the entire accessible electromagnetic (EM) spectrum from radio to GeV and even TeV γ-rays and on all temporal scales from minutes to decades. This temporal variability is essentially stochastic (e.g. Kushwaha et al. 2017b) but there have been occasional claims of QPOs in time series data of blazars in different EM bands. Similar to the temporal variability time-scales, these QPOs apparently have been seen on diverse time-scales ranging from a few tens of minutes to hours to days and even years, although many of these claims are marginal.

Some of the early claims of QPO detections were in the bright blazar OJ 287, where a 15.7-min periodicity in 37 GHz radio observations taken in 1981 April (Valtaoja et al. 1985) and a 23-min periodicity in optical band observations taken in 1983 March (Carrasco, Dultzin-Hacyan & Cruz-Gonzalez 1985) were argued for. A quite convincing ∼11.7 yr QPO was seen using a century long optical data (Sillanpaa et al. 1996) and subsequent flares were predicted in terms of a binary BH model (Valtonen et al. 2008). The blazar S5 0716+714 once seemed to show a QPO period of ∼1 d followed by a weaker period of ∼7 d; these fluctuations were present in both optical and radio bands during a coordinated optical and radio monitoring campaign (Quirrenbach et al. 1991). On another occasion, optical observations of S5 0716+714 also indicated a QPO of period of ∼4 d (Heidt & Wagner 1996). On longer time-scales, five optical outbursts during 1995–2007 were suggested to have a quasi-period of $\sim 3.0 \pm 0.3$ yr (e.g. Raiteri et al. 2003; Foschini et al. 2006; Gupta et al. 2008). For the blazar PKS 2155–304 a possible of QPO of ∼0.7 d was seen with ultraviolet (UV) and

★ E-mail: acgupta30@gmail.com (ACG); ashutosh31tripathi@yahoo.com (AT); wiitap@tcnj.edu (PJW)

optical monitoring using *International Ultraviolet Explorer* (*IUE*) over 5 d (Urry et al. 1993). A peculiar blazar, AO 0235+164, may have shown a QPO of ∼5.7 yr in long-term radio band data (Raiteri et al. 2001).

Over the last decade there have been more claims of detections of QPOs in several other blazars (e.g. Espaillat et al. 2008; Gupta, Srivastava & Wiita 2009; Lachowicz et al. 2009; King et al. 2013; Sandrinelli, Covino & Treves 2014, 2016b; Ackermann et al. 2015; Graham et al. 2015; Bhatta et al. 2016; Sandrinelli et al. 2016a, 2018; Bhatta 2017, 2018; Li et al. 2017; Xiong et al. 2017; Zhang et al. 2017a,b,c; Hong, Xiong & Bai 2018, and references therein), as well as a few other AGNs of different classes (e.g. Gierliński et al. 2008; Lin et al. 2013; Fan et al. 2014; Pan et al. 2016; Zhang et al. 2017d, 2018; Gupta et al. 2018, and references therein), although most of the roughly year-long γ-ray QPO claims are not strong (e.g. Covino, Sandrinelli & Treves 2019).

QPOs in blazars apparently are occasionally present on diverse time-scales in γ-ray, X-ray, optical, and radio bands, where the monitoring data has come from a broad range of space- and ground-based telescopes. Many hundreds of light curves with different time resolutions in different EM bands have been analysed by a variety of groups around the globe and QPOs have been only firmly detected in a few light curves of AGN of different subclasses. We are unaware of a claimed detection of a QPO in the same AGN with a nearly similar central period in the same EM band. Hence is it a logical conclusion that QPOs in AGNs are both rare and transient in nature.

B2 1520+31 ($\alpha_{2000.0} = 15^{\rm h}22^{\rm m}09\overset{\rm s}{.}99$, $\delta_{2000.0} = +31^\circ 44' 14\overset{''}{.}4$ is a high-redshift FSRQ located at $z = 1.49$ (Shaw et al. 2012; Pâris et al. 2017). This blazar was detected in the first three months of *Fermi*-Large Area Telescope (LAT) observations and marked as a variable source (Abdo et al. 2009, 2010c). It has shown daily activity with γ-ray flux in the LAT band $\geq 10^{-6}$ photons cm^{-2} s^{-1} (Cutini & Hays 2009; Sanchez 2010). The broad-band spectral energy distribution (SED) is a typical of FSRQs, with more than an order of magnitude more emission at γ-ray energies than in the optical, so the higher energy bump of the entire spectrum dominates the overall emission (Abdo et al. 2010a). The simultaneous broad-band SED of B2 1520+31 has been investigated (Cao & Wang 2013; Pacciani et al. 2014) and can be explained with a one zone emission model. In considering temporal properties, Kushwaha et al. (2017b) analysed the γ-ray *Fermi*-LAT light curve of this blazar in the energy range 0.1–300 GeV, binned in 3-d intervals. They found that the flux distribution is lognormal, with a linear relation between flux and intrinsic variability. They suggested that the variability is of a non-linear, multiplicative nature and are consistent with the statistical properties of magnetic reconnection powered minijets-in-a-jet model (Biteau & Giebels 2012; Clausen-Brown & Lyutikov 2012). In our study, we also examined the γ-ray light curves of three other bright AGNs (NGC 1275, Mrk 421, and PKS 1510–089). These sources are selected because they were almost continuously detected (>97 per cent) over a data time bin of 3 d (Kushwaha et al. 2017b).

Here we report the first probable QPO detection in the blazar B2 1520+31 with a period of ∼71 d in 0.1–300 GeV γ-ray energies. This is also the first QPO detection in the blazar B2 1520+31 in any EM band at any time-scale.

In Section 2, we briefly describe the γ-ray *Fermi*-LAT data and our analysis procedure. In Section 3, we present the QPO search methods we employed and the results of those analyses. A discussion and our conclusions are given in Section 4.

2 DATA AND REDUCTION

We downloaded γ−ray data for B2 1520+31 for the period between 2008 October 5 and 2015 October 5 (MJD: 54683–57300) from the LAT on board the space-based *Fermi* observatory that was processed through the PASS8 (P8R2) instrument response function. We analysed the data with the *Fermi* Science Tool (v10r0p5) software for photon energies between 100 MeV and 300 GeV. For a given time interval, we first selected the 'SOURCE' class registered events between these energies from a 15° circular region of interest (ROI) centred on the source location (RA: 230.541632, Dec.: 31.737328). At the same time, a maximum zenith angle restriction of 90° was applied to avoid the contamination of γ-rays from the Earth's limb. The corresponding good time intervals (GTIs) were generated using the flag '(DATA_QUAL>0)&&(LAT_CONFIG==1)' that characterizes the spacecraft operation in Scientific mode.

Finally, the effect of selections, cuts, point spread function, and presence of point sources was accounted for in the exposure map, generated on a ROI+10° radius. The input model spectrum XML file of sources within this region was generated using the LAT Third Catalogue (3FGLgll_psc_v16.fit; Acero et al. 2015) that also includes the contribution of Galactic diffuse and isotropic extragalactic emission through the respective emission templates 'gll_iem_v06.fits' and 'iso_P8R2_SOURCE_V6_v06.txt', as provided by the LAT Science Team. Finally, the selected events were optimized against the input model spectrum file and exposure to extract the best-fitting model parameters using the PYTHONimplementation of the 'unbinned likelihood analysis' method (GTLIKE) provided with the software.

We extracted the light curve of the source over every 3-d interval by following the above procedures. The optimization over input source model spectrum file was performed iteratively by removing insignificant sources, measured by test statistics (TS) < 0 and freezing the parameters of low TS sources until convergence is reached (e.g. Kushwaha et al. 2014). All the sources in the model file had the default spectrum from the 3FGL catalogue assumed. Finally, only fluxes $\gtrsim 3\sigma$ defined by a TS of $\gtrsim 9$ were considered, resulting in a ∼97 per cent coverage of the source over the lengthy duration of these observations (e.g. Kushwaha et al. 2017b).

3 LIGHT-CURVE ANALYSIS AND RESULTS

The 0.1–300 GeV *Fermi*-LAT γ-ray light curve of the blazar B2 1520+31, binned in 3 d intervals, for observations taken from 2008 August 5 to 2015 October 5 is plotted in Fig. 1(a). A visual inspection indicated a possible QPO in the observations made during the first portion of this interval (2008 August 5 to 2012 June 22) that are replotted in Fig. 1(b). To examine and quantify the possibility of a QPO, we analysed the nearly 4-yr long light-curve data of Fig. 1(b) employing the extensively used Lomb–Scargle periodogram (LSP) and weighed wavelet Z-transform (WWZ) techniques. In the following subsections, we briefly explain these techniques and the QPO periods detected by them.

3.1 Lomb–Scargle periodogram

The LSP method is widely used to determine if periodicities are present in the data (Lomb 1976; Scargle 1982) and can be applied to unequally sampled data. The method basically involves fitting the sine function throughout the data by using χ^2 statistics. It reduces the effect of the noise on the signal and also provides a measure of the significance of any periodicity it indicates (Zhang et al. 2017a,b,

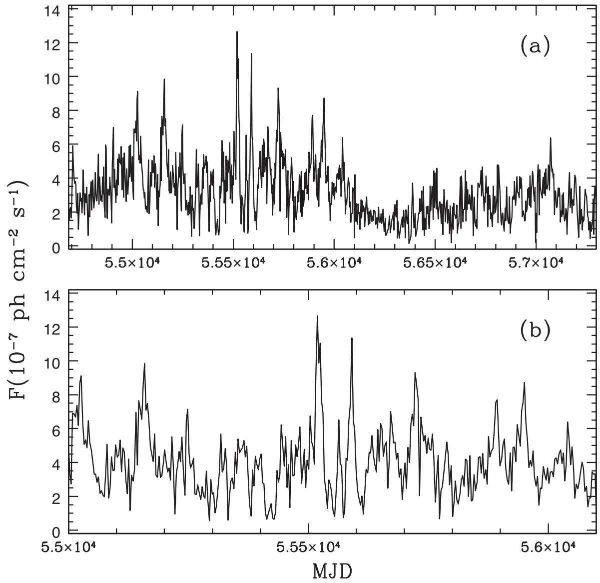

Figure 1. (a) 0.1–300 GeV LAT γ-ray light curve of the blazar B2 1520+31 for data integration times of 3d from 2008 August 5 to 2015 October 5. (b) An expanded segment of the top panel of the light curve taken between 2008 August 5 and 2012 June 22.

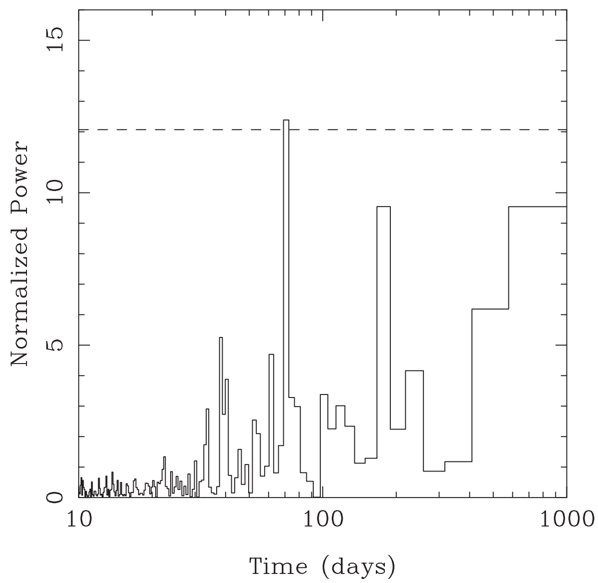

Figure 2. LSP of the light curve in Fig. 1(b). The dashed line represents a null hypothesis or false alarm probability of $p = 0.0001$.

2018; Hong et al. 2018). For more details of our implementation of the LSP, please see Gupta et al. (2018, and references therein).

In Fig. 2, the normalized power of the LSP is plotted against the time period. The horizontal line represents the false alarm probability (FAP) of 0.0001 that corresponds to a nominal 99.99 per cent confidence level. For the power level z, the FAP is given as $p(>z) \approx N \exp^{-z}$, where N is the number of data points (Hong et al. 2018). One signal, at the period of $70.8^{+3.7}_{-2.4}$ d, reached that significance level. This raises the possibility of there being a true QPO of this period that we found to be supported by other methods.

The light curves of AGNs in a range of EM bands from optical through X-rays and γ-rays are usually dominated by red noise,

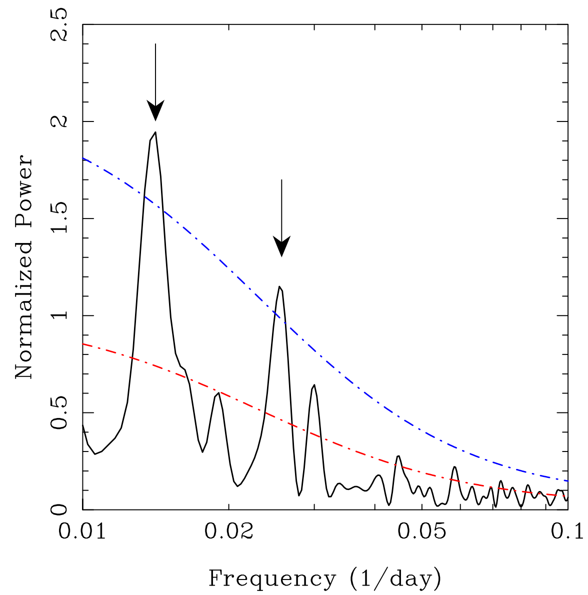

Figure 3. Results of the REDFIT method: the black curve represents the bias-corrected spectra, the red dot–dashed line indicates the computed (AR1) red noise spectrum, and the blue dot–dashed curve shows the 95 per cent χ^2 significance level.

which arises from stochastic processes in the accretion discs, or in the case of blazars, more likely from jets (e.g. Fan et al. 2014; Bhatta 2017; Xiong et al. 2017; Zhang et al. 2017a,c; Hong et al. 2018, and references therein). Blazars generally show power spectrum density dominated by red noise that can be modelled by $P \approx \nu^{\alpha}$, where ν is the frequency and α is the index (e.g. Bhatta et al. 2016). Hence we also employed the REDFIT method to fit the data with a first-order autoregressive (AR1) process (Schulz & Mudelsee 2002; Fan et al. 2014; Xiong et al. 2017; Gupta et al. 2018; Hong et al. 2018). In autoregressive models the data at a given time are related with previous values through a regressive relation, and these can involve different numbers of previous values. In the simplest AR1 model the data point at any instance is taken to be related to just the previous one. This code first computes the time series based on AR1 and generates a theoretical AR1 spectrum. It then calculates significance levels based on the χ^2 distribution. In Fig. 3, the bias-corrected power spectrum and a modelled AR1 spectrum are plotted against the temporal frequency. We find two peaks that are above the displayed 95 per cent significance level. One peak corresponds to the period $70.8^{+1.83}_{-0.73}$ d and the other is at $39.33^{+0.54}_{-0.56}$ d. The second peak could be a harmonic of the first peak, which is more significant. The confidence level is calculated with respect to the computed red noise spectrum. This calculation is based on a reduced χ^2 distribution where the degrees of freedom depend on the number of data points (Schulz & Stattegger 1997; Schulz & Mudelsee 2002).

3.2 Wavelet analysis

Wavelet analyses allow for the determination and estimate of the significance of a period by decomposing the data into time and frequency domains simultaneously (Torrence & Compo 1998), which provide a real improvement over most other techniques. For more details on this approach, see Gupta et al. (2018, and references therein). We used the WWZ[1] software to calculate the WWZ power for a given time and frequency (e.g. King et al. 2013; Bhatta et al. 2016; Bhatta 2017, 2018; Zhang et al. 2017a,b, 2018, and references therein). To estimate the significance of the signal, we also calculate the time-averaged WWZ power, which gives the strength of the signal at each frequency. In wavelet transform, the distribution of power also approaches χ^2 distribution in the limit of even sampling (Foster 1996). The equations for the confidence limits relative to a best-fitting continuum model for periodogram mentioned in Vaughan (2005) also apply here. The difference between periodogram and wavelets, though, is the number of independent trials. The significance is calculated by the method given in Vaughan (2005) for multiple trials.

Fig. 4 shows the results of our WWZ analysis. The left-hand panel of the figure plots the WWZ determined power. It illustrates strong concentrations of power around two periods: $71.43^{+0.51}_{-0.41}$ and $178.57^{+6.25}_{-3.13}$ d. The feature around 71 d is strong and persistent throughout most of the 1400 d considered here, and is exceptionally strong for over seven cycles, an extent rarely if ever seen in other claims for AGN QPOs. The feature at a period of around 179 d is of more moderate strength and is persistent throughout the observation; however, it is both broader and very close to 0.5 yr and thus has a significant chance of being an observational artefact. The time-averaged WWZ powers is plotted in the right-hand panel of Fig. 4 and shows that these periods easily exceed 3σ (99.73 per cent) significance.

4 DISCUSSION AND CONCLUSION

We examined the long-term 0.1–300 GeV energies γ-ray light curves of four AGNs [the Fanaroff–Riley Class I (FR I) radio galaxy NGC 1275, the BL Lac Mrk 421, and the FSRQ PKS 1510–089] and B2 1520+31, as presented in Kushwaha et al. (2017b) to see if they showed any indications of quasi-periodicity. We analysed these light curves using two techniques, LSP (including REDFIT) and WWZ, which are commonly used for searching for QPOs in AGN time series data (Gupta et al. 2018, and references therein). We found a probable QPO with a period of ~71 d in an extended segment of the light curve of the FRSQ B2 1520+31, but did not find a QPO in any of the other three AGNs.

In general, blazar emission across the complete EM spectrum is dominated by non-thermal jet emission. This is primarily because in blazars, the jet is seen at very small angle (<10°) the line of sight to the observer (Urry & Padovani 1995). Jet emission will be strongly amplified due to the relativistic beaming effect, often overwhelming all the thermal contributions from the AGN and the host galaxies stars. But in the FSRQ class of blazars, relatively efficient accretion disc emission and broad-line region (BLR) emission lines are present (D'Ammando et al. 2011). Since B2 1520+31 is a FSRQ, the total emission from this blazar will be expected to have contributions from the accretion disc and the BLR and the jet emission. Many FSRQs show a quasi-thermal excess blue/UV bump above the synchrotron emission in their broad-band SEDs (e.g. Pian et al. 1999; Grandi & Palumbo 2004; Raiteri et al. 2007, 2008; D'Ammando et al. 2009, 2011; Abdo et al. 2010b; Vercellone et al. 2010, and references therein). This portion of the emission from FSRQs is due to both the accretion disc (the so-called 'big blue bump') (e.g. Laor 1990) and the BLR (the so-called 'little blue bump') (e.g. Wills, Netzer & Wills 1985). The contribution of these thermal features will have important consequences in the low-energy part of the SED, in which this emission could be directly observed. Meanwhile, the photons produced by the accretion disc, either directly or through reprocessing in the BLR or the dusty torus, are the source of seed photons for the external Compton (EC) mechanism that is often apparently responsible for the γ-ray emission of FSRQs, which comprises the high-energy hump of the SED and the γ-ray fluxes considered here (e.g. Gaur, Gupta & Wiita 2012; Gupta et al. 2017, Kushwaha et al. 2017a, and references therein).

The mass of the central supermassive black hole (SMBH) in an AGN is, along with the accretion rate and efficiency of mass to energy conversion, one of the most important quantities to characterize. The most accurate, or primary, black hole mass estimation methods include stellar and gas kinematics and reverberation mapping (e.g. Vestergaard 2004). All these methods require high spatial resolution spectroscopy data from the host galaxy and/or higher ionization emission lines and are not applicable to most blazars. The BLL class of blazars have essentially featureless spectra, so primary methods cannot be used. But in the case of FSRQs, prominent emission lines are present, so we can use the method (Vestergaard & Peterson 2006).

An alternative way to estimate the SMBH mass of an AGN comes from using the period of a detected QPO if we assume the QPO is related to the orbital time-scale of a hotspot, spiral shocks, or other non-axisymmetric phenomena in the innermost portion of the rotating accretion disc (e.g. Zhang & Bao 1991; Chakrabarti & Wiita 1993; Mangalam & Wiita 1993; McKinney et al. 2012). Using this assumption for the origin of a QPO, one has an expression for the SMBH mass, M (Gupta et al. 2009),

$$\frac{M}{M_\odot} = \frac{3.23 \times 10^4\, P}{(r^{3/2} + a)(1 + z)}, \qquad (1)$$

in terms of the QPO period P in seconds and the radius of this source zone, r (in units of GM/c^2), and SMBH spin parameter a. The range of nominal masses of the SMBH with such a QPO source can be evaluated in this fashion for perturbations at the innermost stable circular orbit for a Schwarzschild BH (with $r = 6.0$ and $a = 0$), and for a maximal Kerr BH (with $r = 1.2$ and $a = 0.9982$) (Gupta et al. 2009).

In the case of FSRQ B2 1520+31, using equation (1) for the period of 71 d, we get an SMBH mass estimate of 5.41×10^9 M$\odot$ for the Schwarzschild limit and 3.44×10^{10} M$\odot$ for the maximal Kerr limit. Even the former estimate is very large, while the latter exceeds essentially all other SMBH mass estimates (e.g. Dietrich & Hamann 2004; Valtonen, Ciprini & Lehto 2012; Ghisellini et al. 2015; Wu et al. 2015; Zuo et al. 2015), so attributing this apparently detected QPO to emission directly reflecting a transient non-axisymmetric accretion structure is rather unlikely, particularly for the high-energy emission that would not directly emerge from the disc. If the portion of the disc taken to be responsible for a QPO is further out than the innermost portions assumed above, then the estimated mass decreases, perhaps to more reasonable values.

None the less, it is also a prior more likely that the detected QPO in any blazar is related to the jet emission and not directly to that of the accretion disc. If the jet precesses or has an internal helical structure, which is certainly plausible in blazars (e.g. Camenzind & Krockenberger 1992; Villata & Raiteri 1999; Rieger 2004; Mohan & Mangalam 2015), then as shocks advance along the helical structure of the jet or as the jet precesses or twists, quasi-periodic flux variations would arise from variations in the Doppler boosting factor as seen by the observer. Ackermann et al.

[1] https://www.aavso.org/software-directory

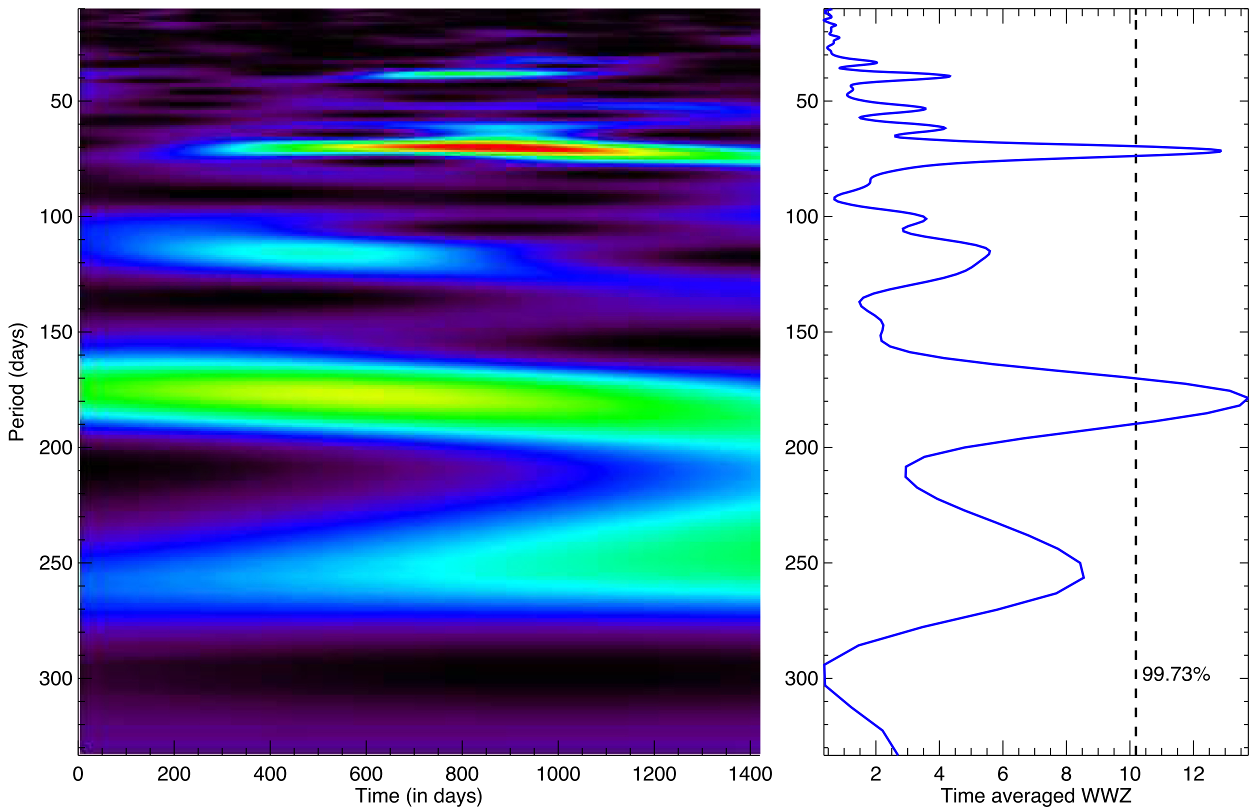

Figure 4. Weighted wavelet Z-transform (WWZ) of the light curve presented in Fig. 1(b). The left-hand panel shows the distribution of colour-scaled WWZ power (with red most intense and black lowest) in the time–period plane; the right-hand panel shows the time-averaged WWZ power (solid blue curve) as a function of period and the 99.73 per cent global significance (dashed black curve).

(2015), in describing a possible roughly 2 yr QPO in the γ-ray (and other band as well) emission from the blazar PG 1553+113, nicely summarize several possibilities along these lines. For instance, Lense–Thirring precession of the disc (e.g. Wilkins 1972) could modulate the direction of the jet (e.g. Fragile & Meier 2009).

Another clear way to induce jet precession is for the AGN to be part of a binary SMBH system (e.g. Begelman, Blandford & Rees 1980; Valtonen et al. 2008; Graham et al. 2015), but these orbits are most likely to produce physical periods in the jets exceeding 1 yr (e.g. Rieger 2007) and several candidate γ-ray QPOs with periods longer than that have recently have been discussed in this framework (e.g. Ackermann et al. 2015; Sandrinelli et al. 2016a,b; Zhang et al. 2017a,b,c). However, as noted by Rieger (2004), the observed periods could be substantially shorter for sufficiently well aligned jets and large enough Lorentz factors. This scenario was shown to be quite reasonable for an apparent QPO in the BLL PKS 2247–131 of an even shorter observed oscillation at around ~34 d (Zhou et al. 2018).

Unfortunately, B2 1520+31 was not the subject of frequent very long baseline interferometry (VLBI) measurements, nor was there good optical monitoring of this blazar between 2008 and 2012. Without a good measurement of the jet Lorentz factor and the angle to our line of sight of the centre of the jet of B2 1520+31, it is not possible to reasonably constrain the parameters of any of these jet-based models to produce the variations in Doppler factors that would be required to yield the high amplitude apparent ~71 d QPO we have found. As the *Fermi* mission remains in good health this object should certainly continue to be examined to see if this or other QPOs are detected.

ACKNOWLEDGEMENTS

This research has used data, software, and web tools of High Energy Astrophysics Science Archive Research Center (HEASARC), maintained by NASA's Goddard Space Flight Center.

We thank the anonymous referee for useful comments that helped us to improve the presentation of the data analysis. ACG thanks Dr W. Atwood for carefully reading the manuscript and a useful comment. AT is thankful to Dr A. Markowitz for discussion about peak significance calculation. ACG is also thankful for hospitality at SHAO, Shanghai, China, during his visit when the draft is written. AT acknowledges support from the China Scholarship Council (CSC), grant no. 2016GXZR89. PK acknowledges support from FAPESP grant no. 2015/13933-0. ZZ is thankful for support from the CAS Hundred-Talented program (Y787081009). CB was supported by the National Natural Science Foundation of China (grant no. U1531117), Fudan University (grant no. IDH1512060), and the Alexander von Humboldt Foundation.

REFERENCES

Abdo A. A. et al., 2009, ApJ, 700, 597
Abdo A. A. et al., 2010a, ApJ, 716, 30
Abdo A. A. et al., 2010b, ApJ, 721, 1425
Abdo A. A. et al., 2010c, ApJ, 722, 520
Acero F. et al., 2015, ApJS, 218, 23
Ackermann M. et al., 2015, ApJ, 813, L41
Begelman M. C., Blandford R. D., Rees M. J., 1980, Nature, 287, 307
Bhatta G., 2017, ApJ, 847, 7

Bhatta G., 2018, preprint (arXiv:1808.06067)
Bhatta G. et al., 2016, ApJ, 832, 47
Biteau J., Giebels B., 2012, A&A, 548, A123
Camenzind M., Krockenberger M., 1992, A&A, 255, 59
Cao G., Wang J.-C., 2013, MNRAS, 436, 2170
Carrasco L., Dultzin-Hacyan D., Cruz-Gonzalez I., 1985, Nature, 314, 146
Chakrabarti S. K., Wiita P. J., 1993, ApJ, 411, 602
Clausen-Brown E., Lyutikov M., 2012, MNRAS, 426, 1374
Covino S., Sandrinelli A., Treves A., 2019, MNRAS, 482, 1270
Cutini S., Hays E., 2009, Astron. Telegram, 2026
D'Ammando F. et al., 2009, A&A, 508, 181
D'Ammando F. et al., 2011, A&A, 529, A145
Dietrich M., Hamann F., 2004, ApJ, 611, 761
Espaillat C., Bregman J., Hughes P., Lloyd-Davies E., 2008, ApJ, 679, 182
Fan J. H., Kurtanidze O., Liu Y., Richter G. M., Chanishvili R., Yuan Y. H., 2014, ApJS, 213, 26
Foschini L. et al., 2006, A&A, 455, 871
Foster G., 1996, AJ, 112, 1709
Fragile P. C., Meier D. L., 2009, ApJ, 693, 771
Gaur H., Gupta A. C., Wiita P. J., 2012, AJ, 143, 23
Ghisellini G., Tagliaferri G., Sbarrato T., Gehrels N., 2015, MNRAS, 450, L34
Gierliński M., Middleton M., Ward M., Done C., 2008, Nature, 455, 369
Graham M. J. et al., 2015, Nature, 518, 74
Grandi P., Palumbo G. G. C., 2004, Science, 306, 998
Gupta A. C., Fan J. H., Bai J. M., Wagner S. J., 2008, AJ, 135, 1384
Gupta A. C., Srivastava A. K., Wiita P. J., 2009, ApJ, 690, 216
Gupta A. C. et al., 2017, MNRAS, 472, 788
Gupta A. C., Tripathi A., Wiita P. J., Gu M., Bambi C., Ho L. C., 2018, A&A, 616, L6
Heidt J., Wagner S. J., 1996, A&A, 305, 42
Hong S., Xiong D., Bai J., 2018, AJ, 155, 31
King O. G. et al., 2013, MNRAS, 436, L114
Kushwaha P., Singh K. P., Sahayanathan S., 2014, ApJ, 796, 61
Kushwaha P., Gupta A. C., Misra R., Singh K. P., 2017a, MNRAS, 464, 2046
Kushwaha P., Sinha A., Misra R., Singh K. P., de Gouveia Dal Pino E. M., 2017b, ApJ, 849, 138
Lachowicz P., Gupta A. C., Gaur H., Wiita P. J., 2009, A&A, 506, L17
Laor A., 1990, MNRAS, 246, 369
Li X.-P., Luo Y.-H., Yang H.-Y., Yang C., Cai Y., Yang H.-T., 2017, ApJ, 847, 8
Lin D., Irwin J. A., Godet O., Webb N. A., Barret D., 2013, ApJ, 776, L10
Lomb N. R., 1976, Ap&SS, 39, 447
McKinney J. C., Tchekhoskoy A., Blandford R. D., 2012, MNRAS, 423, 3083
Mangalam A. V., Wiita P. J., 1993, ApJ, 406, 420
Mohan P., Mangalam A., 2015, ApJ, 805, 91
Pacciani L., Tavecchio F., Donnarumma I., Stamerra A., Carrasco L., Recillas E., Porras A., Uemura M., 2014, ApJ, 790, 45
Pan H.-W., Yuan W., Yao S., Zhou X.-L., Liu B., Zhou H., Zhang S.-N., 2016, ApJ, 819, L19
Pâris I. et al., 2017, A&A, 597, A79
Pian E. et al., 1999, ApJ, 521, 112
Quirrenbach A. et al., 1991, ApJ, 372, L71
Raiteri C. M. et al., 2001, A&A, 377, 396
Raiteri C. M. et al., 2003, A&A, 402, 151
Raiteri C. M. et al., 2007, A&A, 473, 819
Raiteri C. M. et al., 2008, A&A, 491, 755
Remillard R. A., McClintock J. E., 2006, ARA&A, 44, 49
Rieger F. M., 2004, ApJ, 615, L5
Rieger F. M., 2007, Ap&SS, 309, 271
Sanchez D., 2010, Astron. Telegram, 3050
Sandrinelli A., Covino S., Treves A., 2014, ApJ, 793, L1
Sandrinelli A., Covino S., Dotti M., Treves A., 2016a, AJ, 151, 54
Sandrinelli A., Covino S., Treves A., 2016b, ApJ, 820, 20
Sandrinelli A., Covino S., Treves A., Holgado A. M., Sesana A., Lindfors E., Ramazani V. F., 2018, A&A, 615, A118
Scargle J. D., 1982, ApJ, 263, 835
Schulz M., Mudelsee M., 2002, Comput. Geosci., 28, 421
Schulz M., Stattegger K., 1997, Comput. Geosci., 23, 929
Shaw M. S. et al., 2012, ApJ, 748, 49
Sillanpaa A. et al., 1996, A&A, 305, L17
Torrence C., Compo G. P., 1998, Bull. Am. Meteorol. Soc., 79, 61
Urry C. M., Padovani P., 1995, PASP, 107, 803
Urry C. M. et al., 1993, ApJ, 411, 614
Valtaoja E. et al., 1985, Nature, 314, 148
Valtonen M. J. et al., 2008, Nature, 452, 851
Valtonen M. J., Ciprini S., Lehto H. J., 2012, MNRAS, 427, 77
Vaughan S., 2005, A&A, 431, 391
Vercellone S. et al., 2010, ApJ, 712, 405
Vestergaard M., 2004, in Richards G. T., Hall P. B., eds, ASP Conf. Ser. Vol. 311, AGN Physics with the Sloan Digital Sky Survey. Astron. Soc. Pac., San Francisco, p. 69
Vestergaard M., Peterson B. M., 2006, ApJ, 641, 689
Villata M., Raiteri C. M., 1999, A&A, 347, 30
Wilkins D. C., 1972, Phys. Rev. D, 5, 814
Wills B. J., Netzer H., Wills D., 1985, ApJ, 288, 94
Wu X.-B. et al., 2015, Nature, 518, 512
Xiong D., Bai J., Zhang H., Fan J., Gu M., Yi T., Zhang X., 2017, ApJS, 229, 21
Zhang X.-H., Bao G., 1991, A&A, 246, 21
Zhang P.-F., Yan D.-H., Liao N.-H., Wang J.-C., 2017a, ApJ, 835, 260
Zhang P.-F., Yan D.-H., Liao N.-H., Zeng W., Wang J.-C., Cao L.-J., 2017b, ApJ, 842, 10
Zhang P.-F., Yan D.-H., Zhou J.-N., Fan Y.-Z., Wang J.-C., Zhang L., 2017c, ApJ, 845, 82
Zhang P., Zhang P.-F., Yan J.-Z., Fan Y.-Z., Liu Q.-Z., 2017d, ApJ, 849, 9
Zhang P.-F., Zhang P., Liao N.-H., Yan J.-Z., Fan Y.-Z., Liu Q.-Z., 2018, ApJ, 853, 193
Zhou J., Wang Z., Chen L., Wiita P. J., Vadakkumthani J., Morrell N., Zhang P., Zhang J., 2018, Nat. Commun., 9, 4599
Zuo W., Wu X.-B., Fan X., Green R., Wang R., Bian F., 2015, ApJ, 799, 189

This paper has been typeset from a TEX/LATEX file prepared by the author.